J Mater Sci (2011) 46:7649–7659
DOI 10.1007/s10853-011-5742-y

Novel high performance functionalized ladderlike polyphenylsilsesquioxane/bismaleimide hybrids with very good flame retardancy, thermal, and dimensional stability

Dongxian Zhuo · Aijuan Gu · Guozheng Liang · Qian Chen · Tong Chen · Li Yuan · Jiang-tao Hu

Received: 15 May 2011 / Accepted: 22 June 2011 / Published online: 2 July 2011

Abstract Novel high performance hybrids (N-PPSQ/BDM/DBA) with very good flame retardancy, thermal, and dimensional stability as well as low dielectric constant and loss were developed, which consist of 4,4′-bismaleimidodiphenyl methane/2,2′-diallyl bisphenol A (BDM/DBA) resin and a novel functionalized ladderlike polyphenylsilsesquioxane (N-PPSQ). N-PPSQ was synthesized through the hydrolysis and condensation between phenyltrimethoxysilane and γ-aminopropyl triethoxysilane, and its structure was characterized by X-ray diffraction, nuclear magnetic resonance, gel permeation chromatography, and Fourier transform infrared. Compared with BDM/DBA resin, N-PPSQ/BDM/DBA hybrids show significantly improved integrated performances including remarkably reduced dielectric constant and loss, significantly improved flame retardancy, thermal, and dimensional stability, showing great potential for applications having harsh requirements in integrated performances. For example, in the case of the hybrid with 15 wt% N-PPSQ, its coefficient of thermal expansion in glassy and rubbery state are only about 49 and 42% of that of BDM/DBA resin, respectively; its limiting oxygen index increases from about 26.1–42.1%; while its dielectric loss is only about 87% of that of BDM/DBA resin at 1 kHz. These attractive improved properties are attributed to the variety in the cross-linked structure induced by the presence of N-PPSQ.

Introduction

The stability of polymers determines the usage–reliability during the service, and thus attracts great attention of scholars and engineers worldwide [1–3]. In the case of high performance polymers for cutting-edge fields, very good flame retardancy, thermal, and dimensional stability should be their typical and necessary properties [4–6]. However, the stability of most polymers does not completely meet these requirements, especially the flame retardancy. In addition, for a given application, besides these necessary properties, polymers must possess other special properties. For example, low and stable dielectric constant and loss are representative properties of high performance polymers for micro-electric information and electronic insulating industries [7–9]. Therefore, it is of great interest to develop high performance materials with desirable stability in multi-aspects.

Many efforts have been done to improve the stability of polymers [10–12], and achieve valuable results; however, most of them focus on improving the stability of one or two properties [13–15], few of them aims to simultaneously improve the stability of multi-properties because it is a target with great difficulty.

Recently, organic/inorganic hybrids have attracted considerable interest because they combine the advantage of both inorganic and organic materials [16–18]. The principles of hybrids point out that the performance of hybrids is dependent on the properties of inorganic and organic phases as well as the interfacial nature, so these parameters should be carefully designed to exhibit the merits of

---

D. Zhuo · A. Gu (✉) · G. Liang (✉) · Q. Chen · T. Chen · L. Yuan · J. Hu
Jiangsu Key Laboratory of Advanced Functional Polymer Design and Application, Department of Materials Science and Engineering, College of Chemistry, Chemical Engineering and Materials Science, Soochow University, Suzhou 215123, China
e-mail: ajgu@suda.edu.cn

G. Liang
e-mail: lgzheng@suda.edu.cn

hybrids. Many inorganic fillers have been used to prepare various hybrids with some expected properties; however, no inorganic filler has been reported that it can simultaneously endow polymers with increased flame retardancy, improved thermal and dimensional stability as well as decreased dielectric constant and loss.

Polyphenylsilsesquioxane (PPSQ) is a ladderlike polymer, which is also considered as a hybrid because it consists of two –Si–O– main chains bridged by oxygen atoms. Owing to the strong bond energy of Si–O, PPSQ possess outstanding thermal oxidative and dimension stability as well as good insulating properties and moisture resistance [19, 20], so it is expected to develop PPSQ-based hybrids with increased flame retardancy, improved thermal and dimensional stability as well as dielectric constant and loss. In fact, until now, PPSQ has been added to epoxy resin, polystyrene, and polyimide to improve the thermal stability and mechanical properties, and the effect of PPSQ on the properties is not only dependent on the content of PPSQ, but also greatly related to the interface between PPSQ and polymer [21–24]. However, as for the most organic resins, PPSQ generally shows difficulty to be homogeneously dispersed in a polymer because of low reactivity of silanol hydroxyl groups. In order to achieve desirable covalent bonds between PPSQ and a polymer, the PPSQ must be organically functionalized, however, to date, few literatures reported the synthesis of organically functionalized PPSQ, and no work has reported the effect of organically functionalized PPSQ on the integrated performance of a polymer. Therefore, it is greatly interesting to design and synthesize a new PPSQ, which has functional groups and thus good interfacial adhesion with a target polymer.

Thermosetting resins have gained considerable attention owing to their attractive processing characteristics and strong design-ability, so they are considered as the most promising polymers for designing novel advanced composites/hybrids. Bismaleimide (BMI) is known to be the representative thermally resistant thermosetting polyimide [25, 26]. Note that a two-component resin based on 4,4′-bismaleimidodiphenylmethane (BDM) and 2,2′-diallylbisphenol A (DBA) has been proved to have outstanding thermal stability at elevated temperature and retention of properties in hot/wet environments, superior mechanical strength, and toughness as well as good dielectric properties [27]. Therefore, BDM/BDA resin is selected to be the organic phase for developing high performance organic/inorganic hybrids herein.

In order to achieve the target issued in this paper, a new polyphenylsilsesquioxane (N-PPSQ) with functional groups (–NH_2) and ladder structure was designed and synthesized, which is then employed to prepare BDM/BDA resin matrix hybrids. The influence of N-PPSQ on the typical properties (including thermal and dimensional stability, flame retardancy, and dielectric properties) of hybrids was systematically investigated, and that of BDM/BDA resin is also supplied for comparison.

Experimental

Materials

4,4′-Bismaleimidophenyl methane (BDM) was obtained from Fengguang Chemical Co. Ltd (China). 2,2′-Diallyl bisphenol A (DBA) was purchased from Laiyu Chemical Factory (China). γ-Aminopropyl triethoxysilane was supplied by Jingzhou Jianghan Fine Chemical Ltd (China). Phenyltrimethoxysilane was supplied by Zhejiang Chemtech Group Co. Ltd (China). Methanol, potassium acetate, toluene, HCl, and KOH were commercial products with analytical grades, and used without further purification. Distilled water was produced by our lab.

Synthesis of N-PPSQ

Appropriate quantities of phenyltrimethoxysilane and toluene were put into a three-necked flask equipped with a thermometer and condenser, forming a solution. When the solution was cooled to 5 °C with stirring, a certain amount of distilled water containing hydrogen chloride was gradually added into the solution. After that, the reaction mixture was stirred for an additional 3 h, and then transferred to a separation funnel for separation, the reaction mixture became two layers. The lower aqueous layer was removed, and the organic layer was recovered. Distilled water, of which volume is equal to that of the organic layer, was added to the organic layer for washing under shaking, and the same procedure was repeated five times to form a organic solution A.

Next, the organic solution A was transferred into a three-necked flask equipped with a thermometer, condenser, and Dean–Stark trap. Further, a certain amount of a solution B, which was obtained by dissolving KOH in methanol to a concentration of 0.1 mg/mL, was put into the flask and maintained at 100 °C with stirring for 8 h. Subsequently, the mixture solution was added dropwise to methanol (the volume ratio between methanol and the solution is 10:1), and the same procedure was repeated four times, ultimately, to get a white precipitate.

After that, appropriate quantities of white precipitate, potassium acetate, and γ-aminopropyl triethoxysilane were put into a three-necked flask equipped with a thermometer, condenser, and Dean–Stark trap, forming a solution. The mixture was heated slowly with stirring under a nitrogen atmosphere, and the solution was heated to 120 °C and maintained at that temperature with stirring for 2 h.

Subsequently, the solution was added dropwise into methanol (the volume ratio between methanol and the solution is 10:1). Finally, a white solid was obtained, which is polyphenylsilsesquioxane containing –NH_2 groups and coded as N-PPSQ. The schematic synthesis route of N-PPSQ is shown in Scheme 1.

The synthesized N-PPSQ is a white solid, and completely miscible in toluene, tetrahydrofuran, chloroform, etc., suggesting a good processing feature. Its weight-average molecular weight (M_w) is 13897 and polydispersity index is 1.61, revealing that N-PPSQ is a polymer with a low molecular weight and slightly narrow molecular distribution.

Preparation of N-PPSQ/BDM/DBA prepolymer and cured hybrids

Appropriate amounts of BDM, DBA, and N-PPSQ according to each formulation (Table 1) were blended at 135 °C for 30 min with vigorous stirring to obtain a transparent liquid, which was N-PPSQ/BDM/DBA prepolymer.

Each prepolymer was thoroughly degassed to remove entrapped air at 135 °C in a vacuum oven. After that the mixture was cast into a mold for curing and postcuring following the protocol of 150 °C/2 h + 180 °C/2 h + 200 °C/2 h and 230 °C/4 h, respectively. Finally the cured resin was demolded and coded as N-PPSQn/BDM/DBA resin, where n represents the weight loading of N-PPSQ in N-PPSQ/BDM/DBA system, taking the values of 5, 10, 15, and 20.

Preparation of BDM/DBA prepolymer and cured resin

Appropriate amounts of BDM and DBA according to each formulation (Table 1) were blended at 135 °C for 30 min with vigorous stirring to obtain a transparent liquid, which was BDM/DBA prepolymer.

The prepolymer was thoroughly degassed to remove entrapped air at 135 °C in a vacuum oven. After that, the mold was put into an oven for curing and postcuring following the protocol of 150 °C/2 h + 180 °C/2 h + 200 °C/2 h and 230 °C/4 h, respectively, the resultant resin is cured BDM/DBA resin.

Measurements

Fourier transform infrared (FTIR) spectra were recorded between 400 and 4000 cm^{-1} with a resolution of 2 cm^{-1} on a Prostar LC240 Infrared Spectrometer (USA).

^{29}Si-NMR spectra were acquired at 99.36 MHz using 128 scans by a Bruker 500 MHz instrument (Germany). A 5 s delay time was used. ^{29}Si-NMR spectra were acquired with samples in 5 mm (outer diameter) glass cells at 25 ± 2 °C. Chromium(III) acetylacetonate with a concentration of 1% was used as a paramagnetic relaxation agent to promote rapid relaxation of the ^{29}Si nucleus.

Gel permeation chromatography (GPC) measurements were performed at 35 °C with tetrahydrofuran as the eluant (1.0 mL/min) and polystyrene as standards using an Agilent 1100 system (USA).

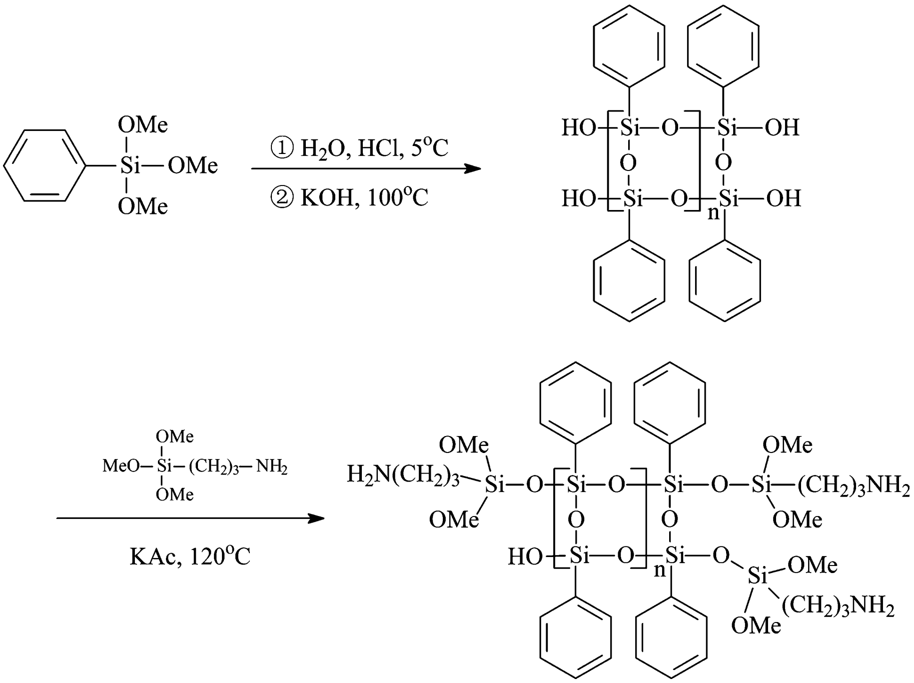

Scheme 1 The synthesis of N-PPSQ

Table 1 Formulations of BDM/DBA resin and N-PPSQ/BDM/DBA hybrids

System	Mass ratio		
	BDM	DBA	N-PPSQ
BDM/DBA	58	42	0
N-PPSQ5/BDM/DBA	58	42	5
N-PPSQ10/BDM/DBA	58	42	10
N-PPSQ15/BDM/DBA	58	42	15
N-PPSQ20/BDM/DBA	58	42	20

X-ray diffraction (XRD) analyses were carried out on a MERCURY CCD X-ray diffractometer (RIGAKu, Japan) with Cu Kα radiation. The 2θ angle ranged from 3° to 70°, and the scan rate was 2°/min.

Differential scanning calorimeter (DSC) measurements were performed with a DSC 2010 (TA Instruments, USA) ranging from room temperature to 320 °C at a heating rate of 10 °C/min under a nitrogen atmosphere.

Thermogravimetric (TG) analyses were performed on a TA Instruments SDTQ600 (USA) in the range from 25 to 900 °C under a nitrogen atmosphere with a flow rate of 100 mL/min and a heating rate of 10 °C/min. The initial decompose temperature (T_{di}) was defined as the point of intersection at which the tangent of onset temperature and the tangent of the maximum degradation rate temperature.

A scanning electron microscope (Hitachi S-4700, Japan) coupled with energy disperse X-ray spectrometer (EDS) was employed to observe the morphology of samples. The resolution of the secondary electron image is 1.5 nm under 15 kV. All samples should be dried at 100 °C for 6 h before test.

Dynamic mechanical analysis (DMA) scans were performed using TA DMA Q800 apparatus from TA Instruments (USA). A single cantilever clamping mode was used. DMA tests were carried out from room temperature to 320 °C with a heating rate of 3 °C/min at 1 Hz. The dimensions of sample were $(35 \pm 0.02) \times (13 \pm 0.02) \times (3 \pm 0.02)$ mm^3.

Coefficient of Thermal Expansion (CTE) was conducted using Thermomechanical Analyzer TMA7 (Perkin Elmer, USA) from 30 to 350 °C with a heating rate of 10 °C/min. Each sample was dried to a constant weight under 110 °C to eliminate the moisture in the sample.

Limiting oxygen index (LOI) values were measured on a Stanton Redcraft Flame Meter according to ASTM D2863/77. The dimensions of sample were $(100 \pm 0.02) \times (6.5 \pm 0.02) \times (3 \pm 0.02)$ mm^3.

The dielectric properties were measured by a Broadband Dielectric Spectrometer (Novocontrol Concept 80, Germany) in the frequency range of 10–10^6 Hz at room temperature. The dimensions of sample were $(25 \pm 0.02) \times (25 \pm 0.02) \times (3 \pm 0.02)$ mm^3.

Flammability of each sample was characterized using a cone calorimeter performed in an FTT device (UK) according to ISO 5660 with an incident flux of 35 kW/m^2 using a cone shape heater. Typical results from cone calorimetry are reproducible to within about ±10%, and the data reported here were the averages of triplicate. The dimensions of sample were $(100 \pm 0.02) \times (100 \pm 0.02) \times (3 \pm 0.02)$ mm^3.

Results and discussion

Synthesis and characterization of N-PPSQ

In order to supply the covalent bond between PPSQ and BDM/BDA resin, those functional groups having good coreaction with bismaleimide should be introduced in the molecules of the new polyphenylsilsesquioxane. As we have known that there is a Michael reaction between maleimide and –NH$_2$ groups (Scheme 2) [28], and several diamine modified bismaleimide resins have been developed for commercial applications [29–31]. Therefore, –NH$_2$ groups are designed to be introduced in the molecule of the new polyphenylsilsesquioxane.

In order to further confirm the molecular structure of N-PPSQ, FTIR, XRD, and ^{29}Si-NMR analyses were carried out. Figure 1 shows the FTIR spectrum of N-PPSQ, it can be seen that the absorption at approximately 1100 cm^{-1} based on –Si–O–Si– stretching vibration clearly splits into two peaks at 1134 and 1047 cm^{-1}, implying the formation of a ladder structure [32]. Moreover, a broad absorption in the range of 3200–3600 cm^{-1} is composed of two components at 3469 and 3373 cm^{-1}, attributing to the characteristic absorptions of Si–OH and –NH$_2$ group, respectively, suggesting that uncondensed Si–OH groups still exist after hydrolysis, and the –NH$_2$ groups are incorporated into the molecules of PPSQ. These results preliminarily prove that the synthesized polysiloxane is a polyphenylsilsesquioxane with ladder structure and reactive –NH$_2$ groups.

XRD diffractograms can provide valuable information about the organization at a molecular level and long-range order. Figure 2 shows the XRD pattern of N-PPSQ, a relatively sharp peak and a very broad peak can be observed at ca. 7° and 19°, respectively, they are attributed to the chain-to-chain distance and intra-chain distances for a stereo-regular double-chain structure called as a ladder structure of PPSQ, respectively [33], hence the appearance of the two peaks demonstrate that N-PPSQ has a structural ordering with a spacing of about 1.3 and 0.5 nm.

Scheme 2 The Michael reaction between maleimide and $-NH_2$ groups

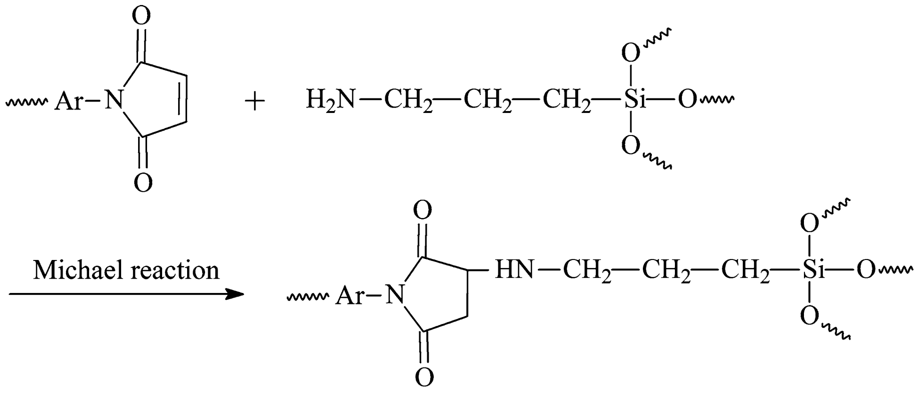

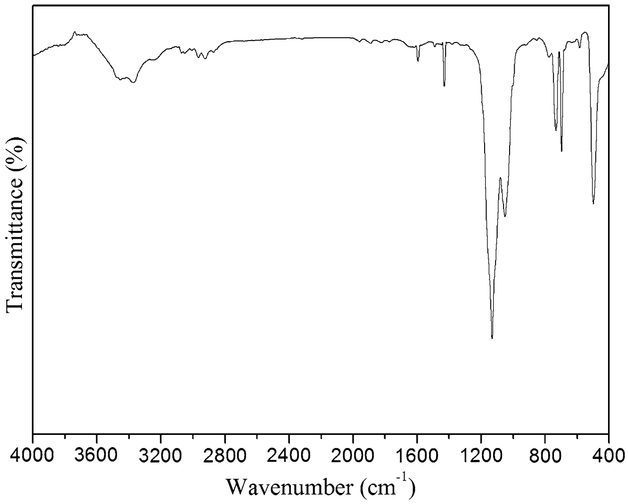

Fig. 1 The FTIR spectrum of N-PPSQ

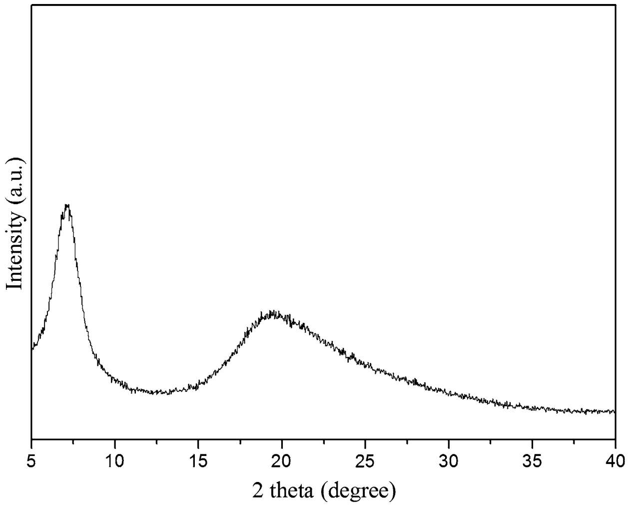

Fig. 2 The XRD pattern of N-PPSQ

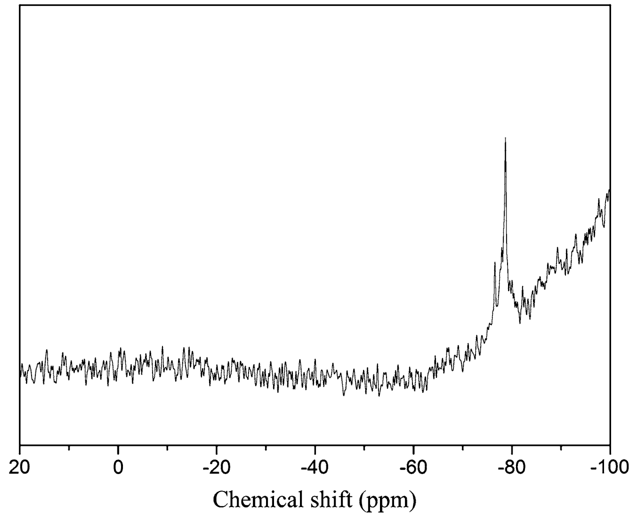

Fig. 3 The ^{29}Si-NMR spectrum of N-PPSQ

The ordered structure of N-PPSQ can be further proved by the ^{29}Si-NMR spectroscopy which provides the information on the structure of the T units. The geminal silane diol (T^1), silanol (T^2), and siloxane (T^3) units could be distinguished by their characteristic chemical shifts. As shown in Fig. 3, the N-PPSQ exhibits two T^3 sites at −78.7 and −76.5 ppm, while no clear signal attributed to a T^2 structure can be observed, reflecting the synthesized N-PPSQ has highly ordered structures [34, 35].

Based on above analyses, it is reasonable to conclude that a novel polyphenylsilsesquioxane with ladder structure and functional $-NH_2$ groups is successfully synthesized.

Thermal stability of cured N-PPSQ/BDM/DBA hybrids

Thermal stability of a material can be reflected by many properties, among them the glass transition temperature (T_g) and TG behavior are two most important ones for high performance resins.

T_g can be tested by some methods, however, the one by defining T_g as the peak (maximum) temperature in the tan delta—temperature plot from DMA measurement is proved to be most effective [36]. Figure 4 shows the overlay plots of tan delta vs. temperature for cured BDM/DBA resin and N-PPSQ/BDM/DBA hybrids. It is noted that all

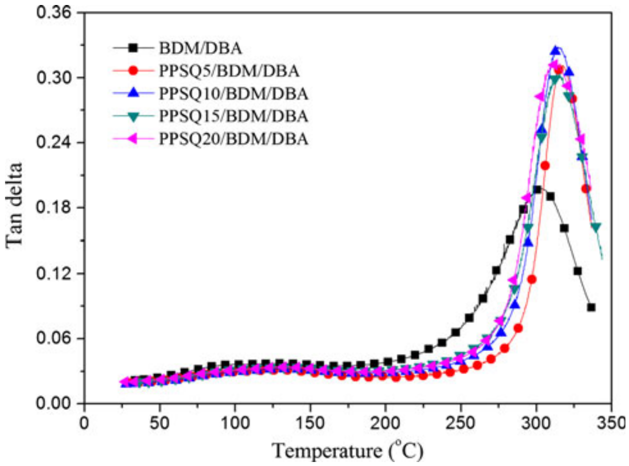

Fig. 4 Overlay curves of tan delta as a function of temperature for cured BDM/DBA resin and N-PPSQ/BDM/DBA hybrids

N-PPSQ/BDM/DBA hybrids have higher T_g values than BDM/DBA resin, demonstrating that the former has significantly improved thermal resistance than the latter. Specifically, the T_g value significantly increases with the addition of only a small amount of N-PPSQ (5 wt%), while which does not further increase with an continuous increasing content of N-PPSQ. These results can be attributed to the effect of N-PPSQ on the crosslinked structure.

As discussed above that there is a Michael reaction between –NH_2 groups in N-PPSQ molecule and double bonds in imide rings of BDM, which not only effectively guarantees the homogeneous dispersion of N-PPSQ in BDM/DBA resin, but also inhabits some segmental motions in the BDM/DBA resin owing to the high rigidity of N-PPSQ, and thus leading to high T_g values. The well dispersion of N-PPSQ in BDM/DBA resin can be confirmed by the Si mapping results of the fracture surfaces of N-PPSQ/BDM/DBA hybrids by EDS analyses as shown in Fig. 5. It can be seen that bright dots assigning to Si atoms homogeneously distribute in each picture, reflecting that N-PPSQ is well dispersed in the resin matrix of N-PPSQ/BDM/DBA hybrids. On the other hand, the Michael reaction also restrains the chain mobility, especially in the network formed by rigid aromatic rings, and thus provides a sterically hindered environment for the reaction between BDM and DBA. Hence, the introduction of N-PPSQ to BMI/DBA resin may hinder further stages of curing reaction between BDM and DBA. This could explain the slightly increased curing temperature observed in the DSC curves of BDM/DBA and N-PPSQ/BDM/DBA hybrids as shown in Fig. 6. This influence ultimately provides a negative role on reducing the T_g values of the resultant curing network. Similar phenomena were also reported in other systems [37, 38]. Obviously, above two influences

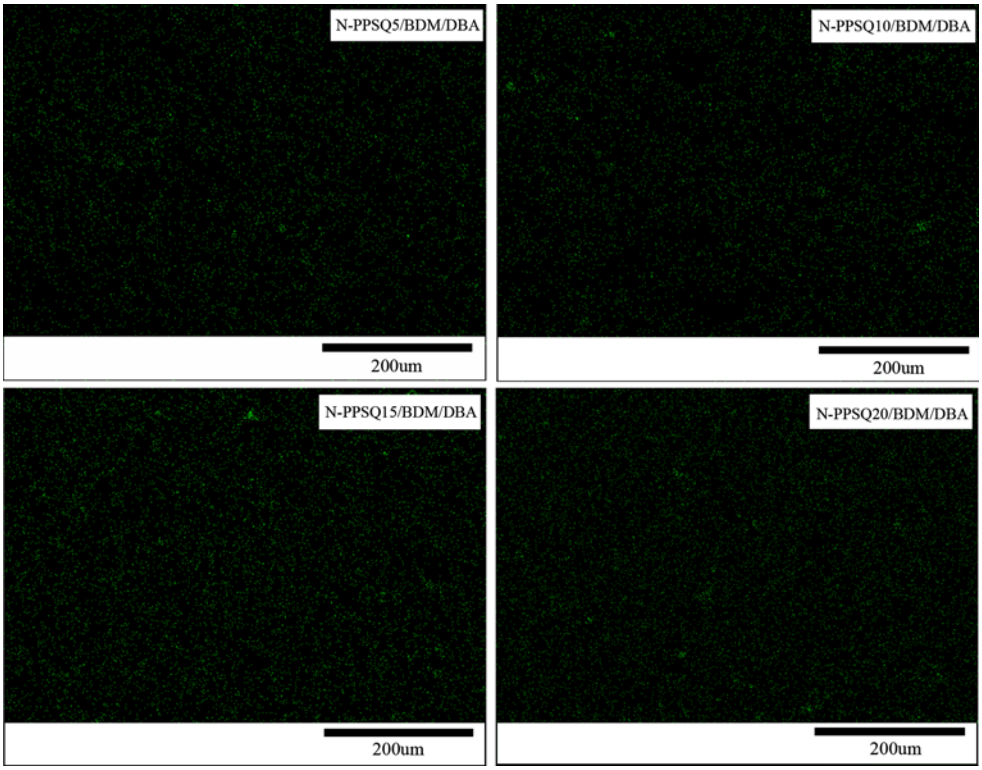

Fig. 5 Si mappings (EDS) of cured BDM/DBA resin and N-PPSQ/BDM/DBA hybrids

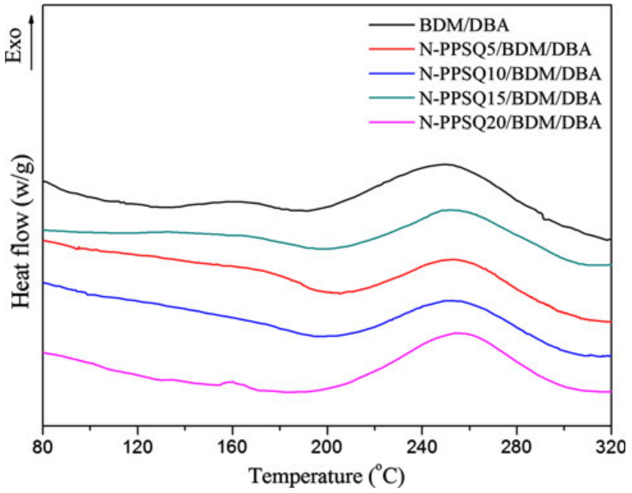

Fig. 6 DSC curves of BDM/DBA and N-PPSQ/BDM/DBA systems

combine together, and thus leading to the phenomena shown in Fig. 4.

The TG behaviors of cured BDM/DBA resin and N-PPSQ/BDM/DBA hybrids were investigated by TG analyses in a N_2 atmosphere, and the corresponding curves are shown in Fig. 7. The typical data, such as initial decompose temperature (T_{di}), the temperature of maximum degradation rate (T_{max}), and char yield (Y_c) at 800 °C, obtained from these curves are summarized in Table 2. It can be seen that all hybrids have similar T_{di} and T_{max} values as BDM/DBA resin does, indicating that they have similar thermal degradation mechanism. Interestingly, compared with BDM/DBA resin, each hybrid has increased Y_c value which increases with the increased content of N-PPSQ resin. Actually, this increase is mainly attributed to the high Y_c value of N-PPSQ resin.

Dimensional stability of cured N-PPSQ/BDM/DBA hybrids

CTE is a very important property in actual applications, which denotes the dimension stability of a material with the variety of service temperature [39]. The CTE values of the BDM/DBA resin and N-PPSQ/BDM/DBA hybrids are shown in Fig. 8. It is interesting to find that the CTE values in both glassy and rubbery states of N-PPSQ/BDM/DBA hybrids clearly show a significant decrease with the increasing content of N-PPSQ. Specifically, with the addition of 15 wt% N-PPSQ to BDM/DBA resin, the linear CTE value in glassy state or rubbery state decreases 51 or 58%, respectively. The attractive decrease is much larger than would be expected with the similar content of other inorganic fillers [40–43], where only 10–30% reductions in CTE value were observed, indicating that N-PPSQ is more effective in enhancing the dimensional stability of bismaleimide resin than traditional organic fillers. On the other

Fig. 7 TG and DTG curves of cured BDM/DBA resin and N-PPSQ/BDM/DBA hybrids in a nitrogen atmosphere

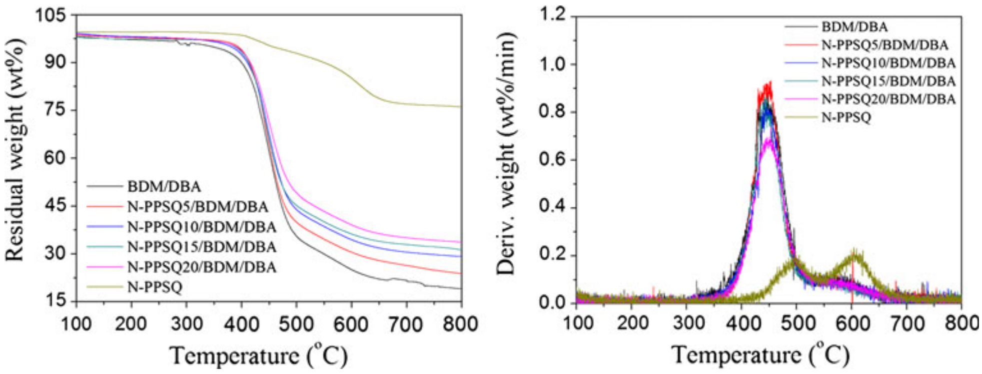

Table 2 Characteristic data from TG analyses of cured BDM/DBA resin and N-PPSQ/BDM/DBA hybrids in a nitrogen atmosphere

System	T_{di} (°C)	T_{max} (°C)		Y_c at 800 °C (wt%)
		T_{max1}	T_{max2}	
BDM/DBA	409.3	441.2	–	19.2
N-PPSQ5/BDM/DBA	413.4	447.2	–	23.2
N-PPSQ10/BDM/DBA	412.7	447.1	–	29.3
N-PPSQ15/BDM/DBA	411.3	441.9	–	31.2
N-PPSQ20/BDM/DBA	412.1	447.8	–	33.7
N-PPSQ	458.6	495.4	614.2	76.3

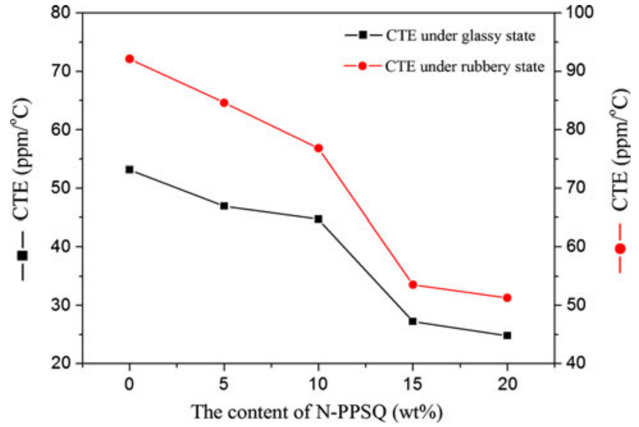

Fig. 8 The CTE values of BDM/DBA resin and N-PPSQ/BDM/DBA hybrids as a function of N-PPSQ loading under glassy and rubbery states

hand, it is interesting to note that the reduction of CTE value is only significant when the content of N-PPSQ is not larger than 15 wt%; while when the content of N-PPSQ is large enough (>15 wt%), the value of CTE decreases slowly and then almost levels off.

The decreased CTE value for N-PPSQ/BDM/DBA hybrids is attributed to following influences. First, N-PPSQ possesses extremely low CTE value because of the existence of a large amount of rigid benzene rings; in addition, the chemical reaction between N-PPSQ and BDM/DBA resin constrains the movement of the polymer network. Second, the sterically hindered environment for the reaction between BDM and DBA as described above tends to increase the CTE value of the resultant network. Obviously, above data prove that the first influence always plays the dominant role, while when the content of N-PPSQ is large enough, the second influence will offset partly the first role, and then the CTE value almost does not further decreases with increasing the content of N-PPSQ.

Controlling CTE is considerably important for multiple materials in applications where polymers are applied to glass, ceramic, or metal substrates with quite dissimilar CTE values. In such applications, thermal cycling often leads to loss of adhesion followed by material failure via chemical and/or mechanical mechanism; on the other hand, CTE mismatch is also quite problematic in electronic applications because which tends to make product deform during the service, and may lead to break down.

It is well known that the excellent processability is the prominent advantage of thermosetting resins comparing with thermoplastic polymers, and thus can meet the harsh requirements of many cutting-edge fields. Note that for above applications, the thermosetting resins should be incorporated with inorganic fillers to get a material of which the CTE value is no larger than 20–30 ppm/°C; however, the concentration of inorganic fillers should be large enough (for example up to 50–70 wt%), while such high level of addition will in turn lead to poor processing characteristics [44, 45]. Attractively, for the N-PPSQ synthesized herein, the addition of a small content of N-PPSQ to BDM/DBA resin can significantly decrease the CTE value, meaning that the resultant N-PPSQ/BDM/DBA hybrids not only maintain the good processability of thermosetting resins, but also have desirable CTE values. These attractive results are useful for actual applications.

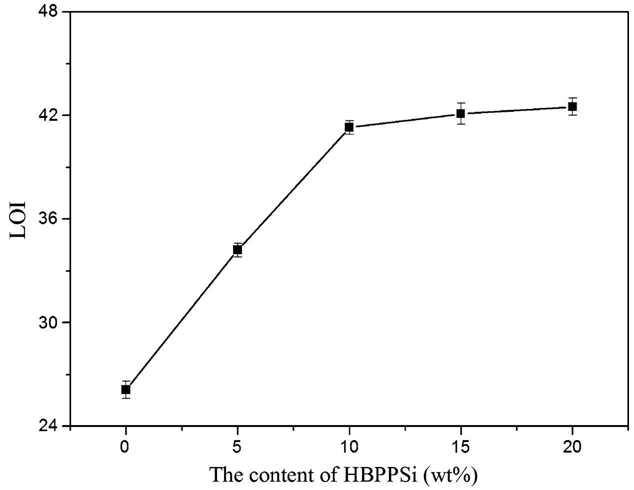

Fig. 9 LOI values of cured BDM/DBA resin and N-PPSQ/BDM/DBA hybrids

Flame retardancy of cured N-PPSQ/BDM/DBA hybrids

LOI and cone calorimeter are two important methods to evaluate the flame retardancy of a polymer. The former quantitatively determines the ability to ignite, while the latter gives the useful information about the burning behavior [46].

Figure 9 shows LOI values of cured BDM/DBA resin and N-PPSQ/BDM/DBA hybrids. All N-PPSQ/BDM/DBA hybrids have significantly higher LOI values than cured BDM/DBA resin. Specifically, with the addition of 10 wt% N-PPSQ to BDM/DBA resin, the LOI value increases from about 26.1–41.3%, indicating that N-PPSQ is an effective flame retardant of BDM/DBA resin. On the other hand, it can be seen that the LOI values of N-PPSQ/BDM/DBA hybrids are closely related with the content of N-PPSQ, however, they do not show a nonlinear relationship. Specifically, the LOI value increases quickly with increasing the content of N-PPSQ when the content of N-PPSQ is below 10 wt%. On the other hand, when the content of N-PPSQ exceeds 10 wt%, the LOI value increases slowly.

Figure 10 shows overlay plots of heat release rate (HRR) vs. time, and those of normalized mass loss vs. time

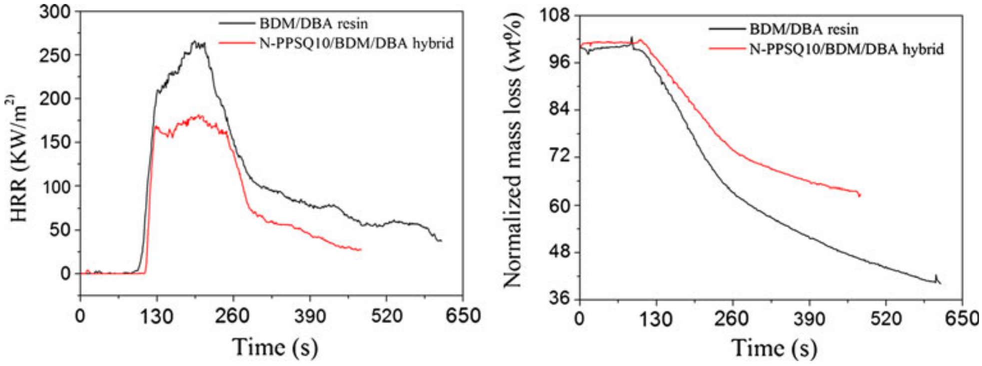

Fig. 10 Dependence of heat release rate and normalized mass loss on combustion time of cured BDM/DBA resin and N-PPSQ10/BDM/DBA hybrid

Table 3 Cone calorimeter data for cured BDM/DBA resin and N-PPSQ10/BDM/DBA hybrid

System	t_{ign} (s)	THR (MJ/m^2)	TSR (m^2/m^2)	PHRR (kW/m^2)	Combustion time (s)
BDM/DBA	89	59.2	2006.3	266.0	613
N-PPSQ10/BDM/DBA	104	34.5	1464.7	181.4	443

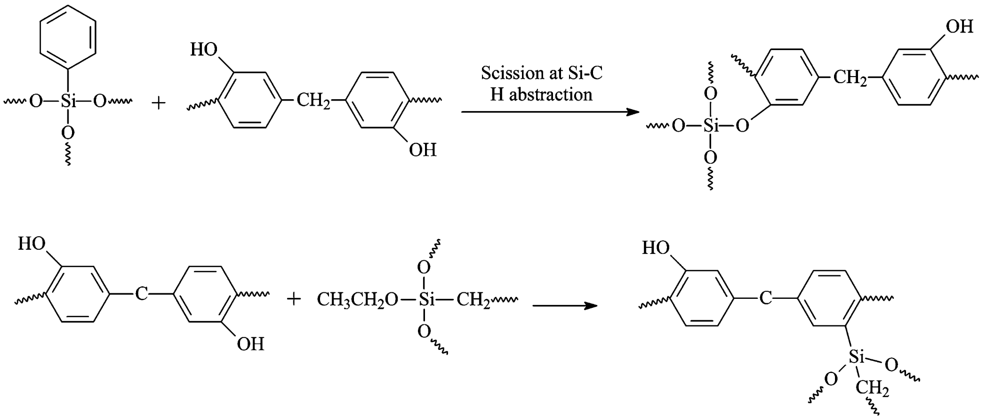

Scheme 3 The flame retarding mechanism of N-PPSQ/BDM/DBA hybrids

for cured BDM/DBA resin and N-PPSQ10/BDM/DBA hybrid; the corresponding data are summarized in Table 3. HRR, including peak heat release rate (PHRR) and total heat release (THR), and the time to ignition (t_{ign}) are three important parameters representing the degree of difficulty in igniting a material. Compared with BDM/DBA resin, the N-PPSQ10/BDM/DBA hybrid displays 32 and 42% reduction in the PHRR and THR, respectively, while its value of t_{ign} lengthens 15 s. The normalized mass loss also follows the similar trend. In addition, the total smoke released (TSR, representing the amount of produced smoke) and combustion time also remarkably reduce with the addition of 10 wt% N-PPSQ10 to BDM/DBA resin, suggesting that the presence of N-PPSQ can not only significantly reduce the HRR, increasing the difficulty in igniting a material, but also effectively inhabit the emission of smoke.

The improvement on flame retardancy can be interpreted by the effect of N-PPSQ on the structure during combustion. Actually, bisphenol groups will attack the carbon-silicon bond in polysiloxane to form a cross-linked structure during the progress of combustion [47–49] (Scheme 3), and thus promote to form a char (Fig. 7) on the surface of the modified resin during combustion, and ultimately not only reducing the radiant heat of flame, but also delaying the volatilization of decomposition products (Fig. 10).

The formation of insulating barrier can be confirmed by the SEM micrographs of the residual chars of cured BDM/DBA resin and N-PPSQ10/BDM/DBA hybrid after combustion as shown in Fig. 11. Compared with the residual char of BDM/DBA resin, that of N-PPSQ10/BDM/DBA hybrid presents a smooth and compact char layer. More interestingly, EDS analyses (Table 4) show that the atom percent of silicon in the exterior and interior of the residual N-PPSQ10/BDM/DBA hybrid is 6.2 and 0.5 wt%, respectively, suggesting that N-PPSQ can be accumulated or pushed by the bubbles on the surface of the resin during

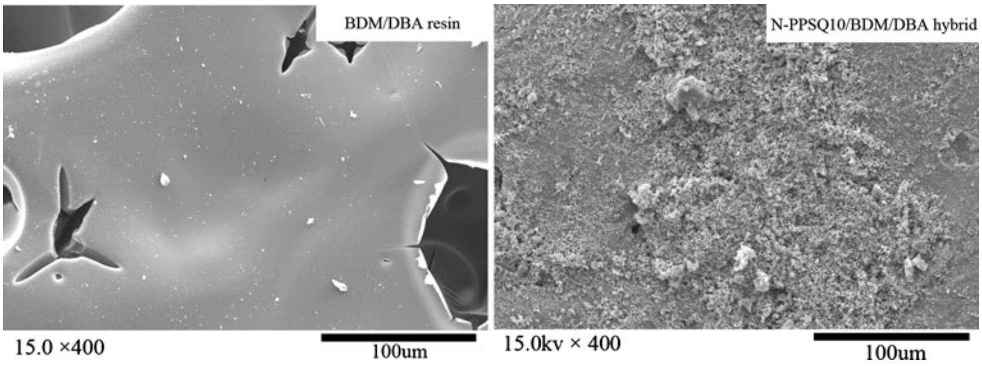

Fig. 11 SEM micrographs of residual chars for cured BDM/DBA resin and N-PPSQ10/BDM/DBA hybrid

Table 4 Elemental compositions of the residual chars for cured BDM/DBA resin and N-PPSQ10/BDM/DBA hybrid by EDS measurements

System	Elemental composition (wt%)			
	C	N	O	Si
BDM/DBA				
Exterior	81.7	9.8	8.5	0.0
Interior	88.5	5.9	5.4	0.0
N-PPSQ10/BDM/DBA				
Exterior	71.7	7.0	15.1	6.2
Interior	78.4	16.0	5.1	0.5

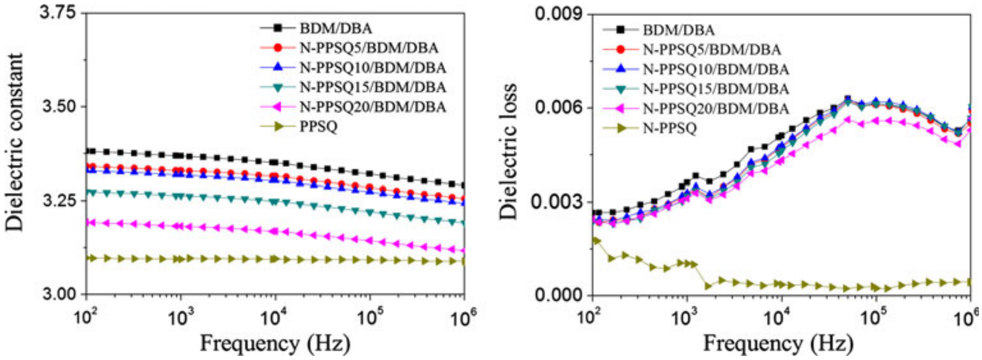

Fig. 12 Dependence of dielectric constant and loss on frequency of cured BDM/DBA resin and N-PPSQ/BDM/DBA hybrids

burning, providing the formation of a continual protective barrier on the surface of modified BDM/DBA resin.

Dielectric properties of cured N-PPSQ/BDM/DBA hybrids

The dielectric constant and loss of cured BDM/DBA resin and N-PPSQ/BDM/DBA hybrids as a function of frequency are shown in Fig. 12. All N-PPSQ/BDM/DBA hybrids exhibit similar stability of dielectric constant and loss over the wide frequency range from 10^2 to 10^6 Hz as neat BDM/DBA resin does; while the former shows attractively lower dielectric constant and loss than the latter, and the larger is the content of N-PPSQ, the lower is the dielectric constant and loss.

Generally, dielectric properties of polymers depend on the orientation and relaxation of dipoles in the applied electric field, the process of dipole polarization accompanies the movement of polymer chain segments [50]. With regard to N-PPSQ/BDM/DBA hybrids, besides the extremely low dielectric constant and loss of N-PPSQ owing to the chemical structure of ladder-like polysiloxane [51], the chemical interaction between N-PPSQ and BDM provides a great restricting influence on the orientation and relaxation of dipoles in the applied electric field, leading to decreased dielectric constant and loss.

Conclusion

A novel ladderlike polyphenylsilsesquioxane with functional –NH_2 groups, coded as N-PPSQ, was successfully synthesized, which can be used to develop a new kind of high performance hybrids. Compared with BDM/DBA resin, N-PPSQ/BDM/DBA hybrids have significantly improved thermal and dimensional stability as well as flame retardancy and dielectric properties, showing great potential for applications having harsh requirements in integrated performance. These attractively improved properties are attributed to the variety in the crosslinked structure induced by the presence of N-PPSQ.

Acknowledgements The authors thank Natural Science Foundation of China (50873073, 20974076), the Priority Academic Program Development of Jiangsu Higher Education Institutions, "Qing Lan Project" (2008), "333 Talent Project" (2011) and "Six Talent Peaks" (2009) of Jiangsu Province for financially supporting this project.

References

1. Zhuo DX, Gu AJ, Liang GZ, Hu JT, Yuan L, Chen XX (2011) J Mater Chem 21:6584
2. Guo QP, Zheng HF, Zheng SX, Mi YQ, Zhu W (1999) J Mater Sci 34:123. doi:10.1023/A:1004486129169
3. Jang J, Nam S, Chung DS, Kim SH, Yun WM, Park CE (2010) Adv Funct Mater 20:2611
4. Chen XL, Yu J, Guo SY, Lu SQ, Luo Z, He M (2009) J Mater Sci 44:1324. doi:10.1007/s10853-009-3273-6
5. Ho TH, Hwang HJ, Shieh JY, Chung MC (2008) Polym Degrad Stab 93:2077
6. Chang CW, Lin CH, Lin HT, Huang HJ, Hwang KY, Tu AP (2009) Eur Polym J 45:680
7. Zhuo DX, Gu AJ, Liang GZ, Hu JT, Yuan L (2011) J Mater Sci 46:1571. doi:10.1007/s10853-010-4964-8
8. Lim H, Chang JY (2010) J Mater Chem 20:749
9. Lin CH, Cai SX, Lin CH (2005) J Polym Sci Polym Chem 23:5971
10. Chen XS, Yu ZZ, Liu W, Zhang S (2009) Polym Degrad Stab 94:1520
11. Modesti M, Lorenzetti A, Besco S, Hrelja D, Semenzato S, Bertani R, Michelin RA (2008) Polym Degrad Stab 93:2166
12. Zhuo DX, Gu AJ, Liang GZ, Hu JT, Zhou C, Yuan L. Polym Adv Technol. doi:10.1002/pat.1814
13. Vothi H, Nquyen C, Lee K, Kim J (2010) Polym Degrad Stab 95:1092
14. Wang X, Hu Y, Song L, Xing WY, Lu HD, Lv P, Jie GX (2010) Polymer 51:2435
15. Deng J, Shi WF (2004) Eur Polym J 40:1137
16. Mackay ME, Tuteja A, Duxbury PM, Hawker CJ, Horn BV, Guan ZB, Chen GH, Krishnan RS (2006) Science 311:1740
17. Belva F, Bourbigot S, Duquesne S, Jama C, Bras ML, Pelegris C, Rivenet M (2006) Polym Adv Technol 17:304
18. Zhu Y, Sun DX, Zheng H, Wei M, Zhang LM (2007) J Mater Sci 42:545. doi:10.1007/s10853-006-1066-8
19. Baney RH, Itoh M, Sakakibara A, Suzuki T (1995) Chem Rev 95:1409
20. Tang HD, Xie P, Zhang RB (2002) J Am Chem Soc 124:10482
21. Li GZ, Ye ML, Shi LH (1996) J Appl Polym Sci 60:1163
22. Li GZ, Wang LC, Toghiani H, Daulton TL, Koyama K, Pittman CUJ (2001) Macromolecules 34:8686
23. Ni Y, Zheng SX (2006) J Polym Sci Polym Chem 44:1093
24. Feng YZ, Qi SL, Wu ZP, Wang XD, Yang XP, Wu DZ (2010) Mater Lett 64:2710
25. Liang GZ, Gu AJ (1997) Bismaleimides. Chem Industry Press, Beijing
26. Hong SG, Yeh CS (2004) Polym Degrad Stab 83:529
27. Li ZM, Yang MB, Huang R, Zhang MD, Feng JM (2001) J Appl Polym Sci 80:2245
28. Liang GZ, Hu XL (2004) Polym Int 53:670
29. Wang CS, Leu TS, Hsu KR (1998) Polymer 39:2921
30. Grenier-Loustalot MF, Cunha LD (1998) Polymer 39:1799
31. Kim DS, Han MJ, Lee JR, Chang JY (1994) Polym Adv Technol 5:287
32. Kim SG, Choi J, Tamaki R, Laine RM (2005) Polymer 46:4514
33. Brown JF, Vogt LH, Katchman A, Eustance JW, Kiser KM, Krantz KW (1960) J Am Chem Soc 82:6194
34. Prado LA, Radovanovic E, Pastore HO, Yoshida IVP, Torriani IL (2000) J Polym Sci Polym Chem 38:1580
35. Matsubara Y, Konishi W, Sugizaki T, Moriya O (2001) J Polym Sci Polym Chem 39:2125
36. Bussu G, Lazzeri A (2006) J Mater Sci 41:6072. doi:10.1007/s10853-006-0694-3
37. Kim KM, Ogoshi T, Chujo Y (2005) J Polym Sci Polym Chem 43:473
38. Li GZ, Jin Y, Shi LH, Ye ML, Bai F (1996) J Polym Sci Polym Phys 34:1079
39. Rashid ESA, Ariffin K, Kooi CC, Akil HM (2009) Mater Design 30:1
40. Wippl J, Schmidt HW, Giesa R (2005) Macromol Mater Eng 290:657
41. Yung KC, Zhu BL, Wu J, Yue TM, Xie CS (2007) J Polym Sci Polym Phy 45:1662
42. Yung KC, Zhu BL, Yue TM, Xie CS (2009) Compos Sci Technol 69:260
43. Sonje PU, Subramanian KN, Lee A (2004) J Adv Mater 36:22
44. Sulaiman S, Brick CM, De SCM, Katzenstein JM, Laine RM, Basheer RA (2006) Macromolecules 39:5167
45. Lu HB, Shen HB, Song ZL, Shing KS, Tao W, Nutt S (2005) Macromol Rapid Commun 26:1445
46. Zenetti M, Camino G, Canavese D, Morgan AB, Lamelas FJ, Wilkie CA (2002) Chem Mater 14:189
47. Lu SY, Hamerton I (2002) Prog Polym Sci 27:1661
48. Zhou WJ, Yang H (2007) Thermochimi Acta 452:43
49. Lji M, Serizawa S (1998) Polym Adv Technol 9:593
50. Fan J, Hu X, Yue CY (2003) J Polym Sci Polym Phys 41:1123
51. Fu JF, Shi LY, Yuan S, Zhong QD, Zhang DS, Chen Y, Wu J (2008) Polym Adv Technol 19:1597